

Observation of large 10-Gb/s SBS slow light delay with low distortion using an optimized gain profile

E. Cabrera-Granado,* Oscar G. Calderón,[†] Sonia Melle[†]
and Daniel J. Gauthier*

*Department of Physics and the Fitzpatrick Institute for Photonics, Duke University, Durham, North Carolina, 27708 USA.

[†] Escuela Universitaria de Óptica, Universidad Complutense de Madrid, C/ Arcos de Jalón s/n, 28037 Madrid, Spain.

ec82@phy.duke.edu

Abstract: An optimum SBS gain profile is designed to achieve better slow-light performance. It consists of a nearly flat-top profile with sharp edges. Tunable delays up to 3 pulse widths for 100-ps-long input pulses, corresponding to 10 Gb/s data rates, are found while keeping an output-input pulse-width ratio below 1.8. Bit-error-rate (BER) measurements performed for a non-return-to-zero modulation format demonstrates 28 ps of delay under error-free operation.

© 2008 Optical Society of America

OCIS codes: (290.5900) Scattering, stimulated Brillouin; (060.4370) Nonlinear optics, fibers; (060.2310) Fiber optics

References and links

1. Y. Okawachi, M. S. Bigelow, J. E. Sharping, Z. Zhu, A. Schweinsberg, D.J. Gauthier, R. W. Boyd, and A. L. Gaeta, "Tunable all-optical delays via Brillouin slow light in optical fiber," *Phys. Rev. Lett.* **94**, 153902 (2005).
2. K. Y. Song, M.G. Herráez and L. Thévenaz, "Observation of pulse delaying and advancement in optical fibers using stimulated Brillouin scattering," *Opt. Express* **13**, 82-88 (2005).
3. D. M. Beggs, T. P. White, L. O'Faolain and T. F. Krauss, "Ultracompact and low-power optical switch based on silicon photonic crystals," *Opt. Lett.*, **33**, 147-149 (2008).
4. B. Zhang, L. S. Yang, J. Y. Yang, I. Fazal, A. Willner, "A Single Slow-Light Element for Independent Delay Control and Synchronization on Multiple Gb/s Data Channels," *IEEE Photon. Technol. Lett.* **19**, 1081-1083 (2007).
5. J. Capmany and D. Novak, "Microwave photonics combines two worlds," *Nature Photon.* **1**, 319-330 (2007).
6. Z. Zhu, A. M. C. Dawes, D. J. Gauthier, L. Zhang, and A. E. Willner, "Broadband SBS slow light in an optical fiber," *J. Lightwave Tech.* **25**, 201-206 (2007).
7. M. González Herráez, K. Y. Song, and L. Thévenaz, "Arbitrary-bandwidth Brillouin slow light in optical fibers," *Opt. Express* **14**, 1395-1400 (2006).
8. K. Y. Song and K. Hotate, "25 GHz bandwidth Brillouin slow light in optical fibers," *Opt. Lett.* **32**, 217-219 (2007).
9. M. D. Stenner and M. A. Neifeld, Z. Zhu, A. M. C. Dawes, and D. J. Gauthier, "Distortion management in slow-light pulse delay," *Opt. Express* **13**, 9995-10002 (2005).
10. T. Schneider, M. Junker, K. U. Lauterbach, and R. Henker, "Distortion reduction in cascaded slow light delays," *Electron. Lett.* **42**, 1110-1111 (2006).
11. Z. Shi, R. Pant, Z. Zhu, M. D. Stenner, M. A. Neifeld, D. J. Gauthier, and R. W. Boyd, "Design of a tunable time-delay element using multiple gain lines for increased fractional delay with high data fidelity," *Opt. Lett.* **32**, 1986-1988 (2007).
12. T. Sakamoto, T. Yamamoto, K. Shiraki, and T. Kurashima, "Low distortion slow light in flat Brillouin gain spectrum by using optical frequency comb," *Opt. Express* **16**, 8026-8032 (2008).
13. Z. Lu, Y. Dong, and Q. Li, "Slow light in multi-line Brillouin gain spectrum," *Opt. Express* **15**, 1871-1877 (2007).

14. L. Yi, Y. Jaouen, W. Hu, Y. Su, and S. Bigo, "Improved slow-light performance of 10 Gb/s NRZ, PSBT and DPSK signals in fiber broadband SBS," *Opt. Express* **15**, 16972-16979 (2007).
15. R. Pant, M. D. Stenner, M. A. Neifeld, and D. J. Gauthier, "Optimal pump profile designs for broadband SBS slow-light systems," *Optics Express* **16**, 2764-2777 (2008).
16. T. Schneider, "Time delay limits of stimulated-Brillouin-scattering-based slow light systems," *Opt. Lett.* **33**, 1398 (2008)
17. T. Tanemura, Y. Takushima and K. Kikuchi, "Narrowband optical filter, with a variable transmission spectrum, using stimulated Brillouin scattering in optical fiber," *Opt. Lett.* **27**, 1552-1554 (2002).
18. J. B. Khurgin, "Performance limits of delay lines based on optical amplifiers," *Opt. Lett.* **31**, 948-950 (2006).
19. A. Zadok, A. Eyal and M. Tur, "Gigahertz-wide optically reconfigurable filters using stimulated Brillouin scattering," *J. Light. Tech.* **25**, 2168-2174 (2007).
20. H. Shalom, A. Zadok, M. Tur, P.J. Legg, W. D. Cornwell and I. Andonovic, "On the Various Time Constants of Wavelength Changes of a DFB Laser Under Direct Modulation," *IEEE J. Quant. Elect.* **34**, 1816-1822 (1998).
21. A. Zadok, A. Eyal, and M. Tur, "Extended delay of broadband signals in stimulated Brillouin scattering slow light using synthesized pump chirp," *Opt. Express* **14**, 8498-8505 (2006).
22. A. Zadok, O. Raz, A. Eyal, and M. Tur, "Optically Controlled Low-Distortion Delay of GHz-Wide Radio-Frequency Signals Using Slow Light in Fibers," *IEEE Photonics Technol. Lett.* **19**, 462-464 (2007).
23. D. Cotter, "Suppression of Stimulated Brillouin Scattering during transmission of high-power narrowband laser light in monomode fiber," *Electron. Lett.* **18**, 638-640 (1982).
24. M. Denariez and G. Bret, "Investigation of Rayleigh wings and Brillouin stimulated scattering in liquids," *Phys. Rev.* **171**, 160-171 (1968).
25. B. Zhang, L. Yan, I. Fazal, L. Zhang, A. E. Willner, Z. Zhu, and D. J. Gauthier, "Slow light on Gbit/s differential-phase-shift-keying signals," *Opt. Express* **15**, 1878-1883 (2007).

1. Introduction

Stimulated Brillouin scattering (SBS) in standard optical telecommunication fibers has proven effective in realizing slow light at room temperature and thus has become a very interesting candidate for all-optical processing in telecommunications networks [1]-[8]. The few pulse widths of delay obtained up to date have shown to benefit tasks such as fast switching [3], clock resynchronization [4] or analog optical processing [5].

In SBS slow light, the delay experienced by the pulses depends on the SBS gain, which is proportional to the pump power and hence can be adjusted in real time. The main drawback of SBS slow light for use in modern communication systems is the inherently small bandwidth of the gain for a monochromatic pump beam, which is ~ 40 MHz in standard optical fibers. This narrow bandwidth translates into large distortion of the delayed pulses for data rates above ~ 40 Mb/s. Thus, broadening the bandwidth to allow transmission of pulses at typical telecommunication data rates of 10 Gb/s without distortion is required.

Stenner *et al.* [9] showed that the frequency-dependent gain (the so-called filtering effect) is the dominant cause for distortion. Furthermore, they showed that distortion can be reduced using two gain lines, which flatten the gain over a finite bandwidth. Different studies have followed this approach to minimize distortion while maximizing the achievable fractional delay. Schneider *et al.* [10] showed a $\sim 30\%$ reduction of the pulse broadening using three different Brillouin gain lines in a two-stage-delay-line. Shi *et al.* [11] showed an increase by a factor of two in the fractional delay at three times larger modulation bandwidth for an optimized triple-gain-line medium as compared with a simple-gain-line. More recently Sakamoto *et al.* [12] used 20 discrete line pump spectra to suppress the broadening factor (defined as the output-to-input pulse-width ratio) to 1.19 for 5.44-ns-long pulses in a two-stage-delay-line. However, all of these approaches are based on the use of a multiple pump spectral lines by means of an external phase or intensity modulator, which limits the maximum bandwidth achievable to a hundred of MHz with present-day commercially-available modulators. The maximum value obtained up to now using this approach is ~ 330 MHz [13].

Larger bandwidths have been obtained by directly modulating the injection current of the pump laser. Herráez *et al.* [7] were the first to demonstrate this effect, broadening a 35 MHz SBS

gain line to 325 MHz. Zhu *et al.* [6] created a 12.6-GHz-wide Gaussian-shaped SBS gain profile by modulating the pump laser current with a Gaussian noise source. They obtained a delay of 47 ps for 75-ps-long input pulses. However, frequency-dependent gain is still present for the Gaussian profile, which causes pulse distortion for large delays. Recently, direct modulation of the pump laser current by a super-Gaussian noise source has been performed by Yi *et al.* [14]. They showed that the filtering effect is reduced with this scheme because the edges of the gain profile are sharpened. Their experiments showed a maximum time delay of 35 ps for a 10 Gb/s NRZ signal with error-free operation.

Optimization of a broadband gain profile has been conducted theoretically by Pant *et al.* [15] to determine the SBS gain profile that minimizes distortion under the constraint of a maximum available pump power. They found that the optimum profile is essentially a flat-top gain spectrum with sharp edges, surrounded by narrow absorption features for bandwidths below 7 GHz. Above 7 GHz, the absorption features are no longer needed. Their calculations reveal an increase in delay by a factor of 1.3 in comparison to a Gaussian-shaped gain profile for a fixed pump power and allowed pulse distortion. More recently, Schneider [16] obtained essentially the same results, showing an enhancement of the time delay when two narrow losses are superimposed at the wings of the gain. Khurgin [18] also show an improvement in the delay performance with distortion constraints when the gain is flattened. Moreover, Tanemura *et al.* [17] and Zadok *et al.* [19] also designed flat-top SBS gain profiles to obtain low-distortion narrow-band filters for microwave photonic applications with 3-dB bandwidths up to 2.5 GHz.

Here, we develop a systematic procedure to minimize distortion while maximizing pulse delay for data rates of 10 Gb/s, which has not been addressed by other studies to the best of our knowledge. We approach this task by generating an optimum broadband SBS gain profile, which, according to the discussion above, consists of a nearly rectangular spectral profile. The procedure described in this work can be easily generalized to any DFB laser used as the pump in SBS slow-light experiments. Although, as it has been mentioned before, a super-Gaussian profile has already been obtained using a super-Gaussian noise distribution to modulate the injection current [14], the procedure performed in our work allows one to obtain a wider gain profile with sharper edges for a given modulation amplitude.

In order to fulfill this goal, we directly modulate the laser injection current with an optimized waveform. To obtain the optimum profile, we start with a waveform that accounts for the transient behavior of the instantaneous pump laser frequency, following the work of Shalom *et al.* [20]. This approach has also been used by Zadok *et al.* [21, 22] to design a pump spectrum with sharp edges. In particular, in Ref. [21] they showed an increase in the delay by a factor of 30% for 270-ps-long pulses, compared with random modulation of the pump laser injection current. However, the gain profiles they obtained deviate substantially from a flat-top profile. On the other hand, the results in our approach, we measure the transient behavior of the pump laser frequency for a step change in the injection current and use this information as the input to an iterative scheme that allows us to obtain an optimum spectral profile.

The paper is organized as follows. Section II describes the procedure to obtain the flat-top SBS gain profile, and accounts for the results. Section III describes the delay performance for 100-ps-long pulses and quantifies the pulse distortion by the output-to-input pulse-width ratio. Section IV shows the BER measurements for a 10 Gb/s non-return-to-zero (NRZ) data format and the maximum delay achieved with error-free operation. Finally, Section V summarizes our main conclusions.

2. Experimental design of the optimal SBS gain profile

It is well known that modulating the injection current of DFB lasers causes the frequency of the output light to change, which has been used extensively to broaden the pump spectrum [23].

The resultant SBS gain spectrum is then given by the convolution of the pump spectrum with the complex gain of the medium [24], which has a Lorentzian profile. To design an optimum broadband SBS gain profile, we must generate a suitable pump spectrum and hence tailor the injection current waveform.

The frequency chirp of the laser beam under current modulation has two main contributions, as described in Ref. [20]. The first is called adiabatic chirp, which is associated with the effect of the injection current on the index of refraction of the laser cavity. It follows almost instantaneously the current variation and increases the laser frequency for an increasing current. The second contribution is a thermal chirp. A sudden increase of the injection current is followed by a slower temperature increase, which modifies the index of refraction and hence the frequency. This frequency variation has an exponential time dependence under a step change of current and is opposite to the adiabatic chirp. The time constants that describes this frequency change depend on the thermal constants of the different layers of the laser, and can be as fast as a few nanoseconds [20]. Therefore, even for fast modulation of the injection current, an analysis of these time constants and the adiabatic chirp is necessary to obtain a precise design of the laser spectrum.

To obtain an optimized waveform for modulating the pump laser current, we generalize the semi-empirical model introduced in Ref. [20]. In particular, we assume that the change of the instantaneous frequency under a current variation is given by

$$v(t) - v_0 = \alpha[i(t) - i_0]^2 + \beta[i(t) - i_0] - h_T \otimes [i(t) - i_0]. \quad (1)$$

Here, the first two terms on the right-hand-side of Eq. 1 account for the adiabatic chirp, where we have included a nonlinear contribution with coefficient α . This is the first time that a nonlinear dependence on the injection current has been considered to the best of our knowledge. We will show below that this contribution must be taken into account to design an optimum slow-light channel at bandwidths exceeding a few GHz. The coefficient β measures the usual linear adiabatic chirp, as described in Ref. [20]. Both α and β are parameters describing a particular DFB laser, while v_0 is the reference frequency value for a background injection current i_0 . The modulation waveform of the current is given by $i(t)$. The thermal chirp is described by the convolution between the injection current with the impulse response of the thermal chirp h_T , which is given by

$$h_T = \sum a_n e^{-t/\tau_n}. \quad (2)$$

We measure the frequency chirp by beating the modulated pump laser beam with a second unmodulated beam generated by an auxiliary laser. If $i(t)$ takes the form of a step function, the beat frequency undergoes a sudden change followed by an exponential decay to a stationary value Δv_{st} . While the thermal chirp is responsible for the exponential decay, the adiabatic chirp determines Δv_{st} where the contribution of the last term in Eq. 1 tends to zero for a step change in $i(t)$. Figure 1 shows Δv_{st} as a function of the step amplitude $i - i_0$ for a pump laser used in one part of our experiments (Sumitomo Electric, model STL4416), where a substantial quadratic dependence is visible. By fitting the adiabatic-chirp part of Eq. 1 to the data, we find $\alpha = 0.0013$ GHz/mA² and $\beta = 0.36$ GHz/mA.

To obtain the values of the parameters a_n and τ_n that characterize the thermal chirp, we measure the total chirp produced by a step change in $i(t)$. According to Eqs. (1) and (2) the thermal chirp leads to a multi-exponential decay of the beat frequency. Therefore, we can obtain the values of a_n and τ_n by fitting the temporal evolution of the frequency to a sum of exponentials. We find that the dominant contributions to the thermal chirp can be captured using three time constants, whose values are given in Table 1. Note that the dominant term has a rather fast time constant of only 7.5 ns.

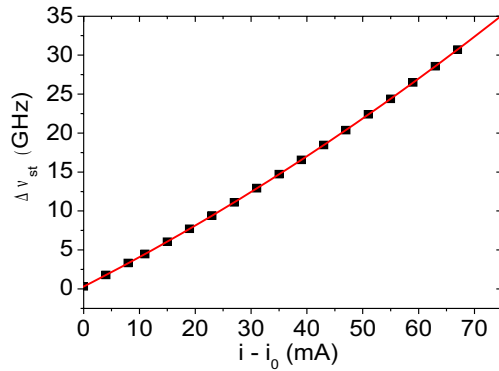


Fig. 1. Adiabatic frequency chirp of the Sumitomo laser. Experimentally measured (solid squares) stationary values of the frequency shift as a function of the step change in the injection current $i - i_0$. Fit to the data (solid line) using the function $\Delta\nu(t) = 0.29 \text{ GHz} + 0.36 \text{ GHz/mA} \cdot (i - i_0) + 0.0013 \text{ GHz/mA}^2 \cdot (i - i_0)^2$, where i_0 is 30 mA.

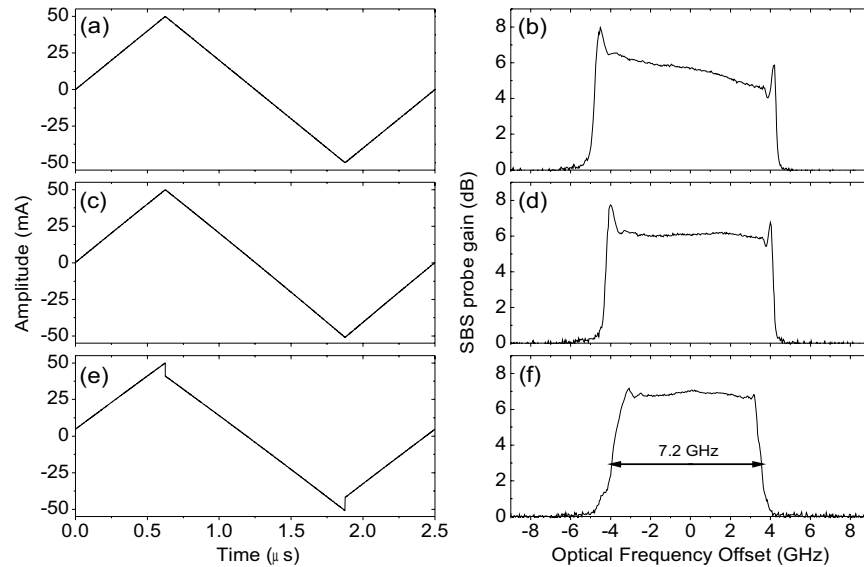


Fig. 2. Modulation waveform (left column) and measured SBS gain profile (right column) for triangular modulation (upper row), with the addition of the quadratic term (middle row), and for the optimum waveform (lower row). Here, $i_0 = 90 \text{ mA}$.

j	1	2	3
a_j (GHz/mA)	0.14	0.013	0.001
τ_j (ns)	7.5	46	190

Table 1. Time constants and coefficients of the impulse response of the thermal chirp.

To optimize the SBS gain spectrum, we modulate initially the injection current with a triangular function with amplitude $\Delta i_{max} = 50$ mA (see Fig. 2(a)), generated by an arbitrary waveform generator (Tektronix, AFG3251). There is a great latitude in choosing the modulation period T . It must be much shorter than the transit time of light through the optical fiber that serves as the slow light medium (10 μ s in our case). On the other hand, longer T produces a broader spectrum for a given injection current. We choose $T = 2.5$ μ s.

Figure 2(b) shows the measured SBS gain profile using the triangular modulation waveform with $i_0 = 90$ mA. It is seen clearly that the resultant gain profile is asymmetric. To explain this behavior, we calculate the time derivate of the adiabatic frequency chirp, which indicates, in first approximation, the time spent at each frequency in one period. A nearly constant value of this derivative is required to achieve a flat spectrum profile. For the sake of simplicity, we focus on the semi-period $[T/4, 3T/4]$ as the frequency goes through the whole range of possible values. The value of the derivative is $d\Delta v(t)/dt = -(4/T)\Delta i_{max}[2\alpha\Delta i_{max}(2 - 4t/T) + \beta]$. This expression clearly shows a linear dependence on time due to the presence of the nonlinear adiabatic chirp, which causes the asymmetry shown in the gain profile. The maximum variation of this term is $16\alpha\Delta i_{max}^2/T$, which is almost 50% of the maximum value of $d\Delta v(t)/dt$ for these laser parameters. This result shows that the nonlinear term of the adiabatic chirp is affecting substantially the slow light performance at large bandwidths where high current modulation amplitudes are used.

Correcting this asymmetry can be accomplished by adding a small quadratic term to the triangular waveform, which results in the SBS gain lineshape shown in Fig. 2(d). The modulation function is then given by

$$i(t) = \Delta i_{max} \begin{cases} at^2 + (4/T - aT/4)t & \text{if } t \leq T/4 \\ at^2 - (4/T + a3T/4)t + 2 + 2aT^2/4^2 & \text{if } T/4 < t \leq 3T/4 \\ at^2 + (4/T - a9T/4)t + 5aT^2/4 - 4 & \text{if } 3T/4 < t \leq T. \end{cases} \quad (3)$$

The optimum value of the quadratic coefficient a can be obtained by applying an iterative scheme. First, we estimate a value of a based on the knowledge of the adiabatic chirp coefficients. With the modulation waveform given by Eq. 3, the time derivative of the adiabatic frequency chirp can be approximated by a parabolic dependence on time

$$\begin{aligned} \frac{d\Delta v(t)}{dt} &\simeq -\frac{12\alpha a\Delta i_{max}^2}{T}t^2 + \Delta i_{max} \left(\frac{16\alpha\Delta i_{max}}{T^2} + a\beta + 10a\Delta i_{max}\alpha \right) t \\ &- \Delta i_{max} \left[\beta \left(\frac{4}{T} + \frac{3aT}{4} \right) + 16\alpha\Delta i_{max} \left(\frac{1}{T} + \frac{aT}{4} \right) \right], \end{aligned} \quad (4)$$

where quadratic terms in a has been neglected. To minimize the variation of this derivative, the center of the parabola is chosen to be at the center of the time interval, *i.e.* $t = T/2$. This condition allows us to obtain the estimated $a \simeq -(16/T^2)\alpha\Delta i_{max}/(\beta - 2\alpha\Delta i_{max})$, which gives $a \simeq -3.4 \times 10^{-7}$ ns⁻². Starting from this value, we make small changes in a while the resultant

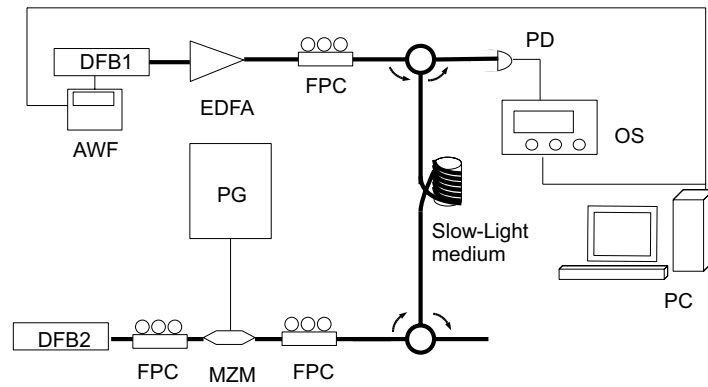


Fig. 3. Experimental setup. The pump laser (DFB1) is modulated by the optimal waveform using an arbitrary waveform generator (AWF) which is computer-controlled. The Er-doped fiber amplifier (EDFA) is used to increase the pump power. Fiber polarization controllers (FPC) are used to match the polarizations of the pump and the signal. The pulses are generated by a pattern generator (PG) that drives a Mach Zehnder Modulator (MZM) placed after the signal laser (DFB2). A photodetector (PD) and a 50-GHz bandwidth sampling oscilloscope (OS) are used to record the pulses.

gain profile is measured for each value. We then compare this profile to an optimum flat-top spectrum by calculating the error as the 2-norm of the difference. After a small number of iterations, a minimum value of the error is obtained, which gives us the optimum value of a_{opt} . Note that the value of the quadratic coefficient depends on the particular laser used. For the Sumitomo laser, $a_{opt} = -2.5 \cdot 10^{-7} \text{ ns}^{-2}$, which is close to our initial estimate.

Although the asymmetry of the gain profile is removed for the case shown in Fig. 2(d), there are still narrow gain peaks at the edge of the profile that can cause pulse-distortion for large bandwidths. These peaks appear because more time is spent by the instantaneous laser frequency in these regions due to the thermal chirp. They can be removed by adding small jumps to the maximum and minimum values of the modulation waveform. Then, a constant term $-\Delta i_{max} d_2$ for $T/4 < t \leq 3T/4$, and a term $\Delta i_{max} 4d_3(1 - t/T)$ for $3T/4 < t \leq T$ must be added to Eq. 3. The value of the parameters d_2 and d_3 can be obtained following the same iterative scheme performed to obtain the value of the quadratic coefficient a . In the case of the Sumitomo laser, $d_2 = 0.158$ and $d_3 = 0.04$. Figure 2(f) shows the final SBS gain profile, with a bandwidth of 7.2 GHz, obtained with the final modulation waveform shown in Fig. 2(e) and for $\Delta i_{max} = 50 \text{ mA}$. This systematic procedure to obtain the optimum current modulation waveform can be applied to any DFB laser, where the free parameters a, T, d_2 and d_3 depend on the frequency chirp properties of the particular laser.

We note that modulating the injection current modulates power in addition to modulating the frequency, which can influence the total pump power spectrum. However, numerical simulations show that the power modulation has little effect on the spectrum for the modulation waveform used in the experiment. This can be explained by the relatively long value of T used in the experiment, which makes the spectral changes due to power modulation occur over a much narrower frequency range in comparison to the frequency excursion due to the thermal and adiabatic chirp.

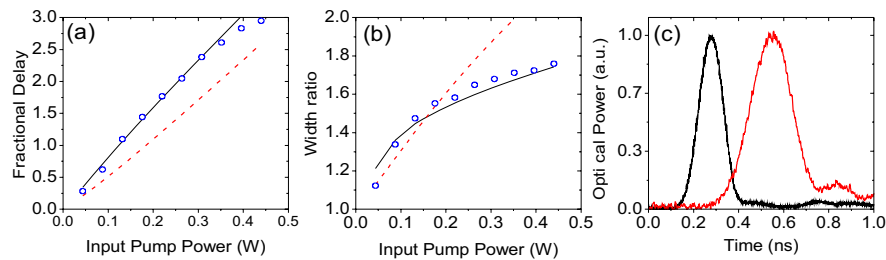


Fig. 4. (a) Fractional delay vs input pump power for experimental data (blue circle) and simulations for the optimal gain profile (black line) and Gaussian gain profile (red dashed line). (b) Output-to-input pulse-width ratio for experimental data (blue circle) and simulations for optimal profile (black solid line) and Gaussian gain profile (red dashed line) (c) Reference pulse (black line) and delayed pulse (red line) for 360 mW showing a fractional delay of 2.6 and an output-to-input pulse-width ratio of 1.7.

3. Slow light performance

The experimental setup is depicted in Fig. 3. We use a 2-km-long Highly Nonlinear Fiber (OFS) that has a smaller effective modal area and thus a higher SBS gain for a given input power in comparison to a standard single-mode fiber. A high-power Erbium-doped fiber amplifier (IPG, EAD-1K-C) provides enough pump power to obtain appreciable gain. Two identical DFB lasers (Sumitomo Electric, STL4416) are used as the pump and the probe lasers and the necessary frequency tuning is achieved by controlling the temperature of each laser. The pump spectrum is broadened by injecting the optimized waveform previously described into the pump-laser drive current using a 50 Ω -impedance bias-T. The signal pulses are created by amplitude modulating the output of the probe laser with a Mach-Zehnder modulator, which is driven by a pattern generator. The data pulses are measured with a 50-GHz bandwidth digital sampling oscilloscope.

The delay performance is improved with respect to the Gaussian gain profile, as predicted in Ref. [15]. Figure 4(a) shows the experimental fractional delay, defined as the ratio between the time delay and the full width at half maximum (FWHM) of the input pulses. A maximum value of 3 is achieved for a single pulse with an input pulse width of 100 ps and a pump power of ~ 440 mW. Figure 4(b) shows the output-to-input pulse-width ratio, which remains below 1.8 for the range of input pump powers used. The simulated results, obtained using the undepleted pump approximation [15], can be seen in the same graphs for the simulated optimal profile, showing a good agreement with the experimental results. For the sake of comparison, we also show the simulated results with a Gaussian gain profile of the same FWHM and total pump power as the simulated optimum gain profile. The experimental results for the fractional delay shows an improvement of 1.3 times the simulated results for a Gaussian gain profile. The distortion for the optimum gain profile is also reduced by a factor of 1.2 at high gains with respect to the Gaussian profile.

Lower broadening factors may be needed for application in telecommunication transmission at 10 Gb/s. This could be achieved by increasing the pump spectrum bandwidth up to 10 GHz. Unfortunately, the laser described in the previous section does not reach this bandwidth for the available injection current Δi_{max} . In order to fulfill this goal, we use another DFB laser as the pump laser (Fitel, FOL15DCWC-A82-19340-B). The previous procedure is repeated to obtain the optimum modulation waveform for this laser. In this case, the adiabatic chirp coefficients are $\alpha = 0.0012$ GHz/mA² and $\beta = 0.35$ GHz/mA, which are similar to the Sumitomo laser

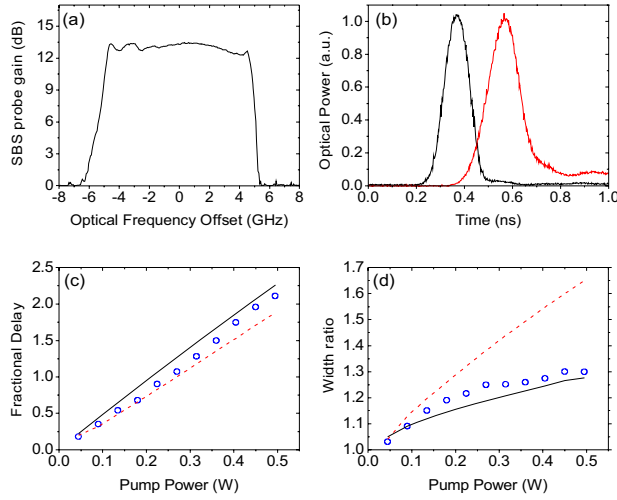


Fig. 5. (a) Gain profile of 9.2 GHz of bandwidth obtained using the Fitel laser with chirp parameters in Table 2. (b) Reference pulse (black line) and delayed pulse (red line) for a pump power of 495 mW. The fractional delay is 2.1 and the output-to-input width ratio is 1.3. (c) Fractional delay vs. input pump power for 100-ps-long pulses. (d) Output-to-input width ratio vs input pump power. Simulations for an optimum flat-top gain profile (black line) and for a Gaussian profile (red dotted line) are also shown.

parameters. The coefficients and time constants of the thermal chirp are shown in Table 2. We choose the same period $T = 2.5 \mu\text{s}$ for the modulation waveform, and the new parameters for the optimum waveform are $a = 1.5 \cdot 10^{-7} \text{ ns}^{-2}$, $d_2 = 0.12$, $d_3 = 0.09$, and $i_0 = 200 \text{ mA}$. Figure 5(a) shows the flat-top gain profile obtained with this pump laser with a bandwidth of 9.2 GHz.

j	1	2	3
a_j (GHz/mA)	0.1	0.5	0.3
τ_j (ns)	16	52	200

Table 2. Time constants and coefficients of the impulse response of the thermal chirp for the Fitel laser.

Using this broader-bandwidth flat-top gain profile, the distortion can be reduced. However, the delay is also reduced because the SBS gain is lower at this broader bandwidth at a given laser power. Figure 5(a) shows the delay as a function of the pump power, while Fig. 5(b) shows the measured output-to-input width ratio. A delay of 2.1 pulses with a broadening factor of 1.3 has been achieved.

4. BER measurements

The designed SBS gain spectrum is optimized for single-pulse propagation [15]. To assess its behavior in communication applications we propagate a high data-rate stream of pulses through our system. We measure the bit-error-rate (BER) performance for a 2^7-1 10-Gb/s NRZ pseudo-random bit sequence (PRBS) and measure the maximum delay achieved with error-free opera-

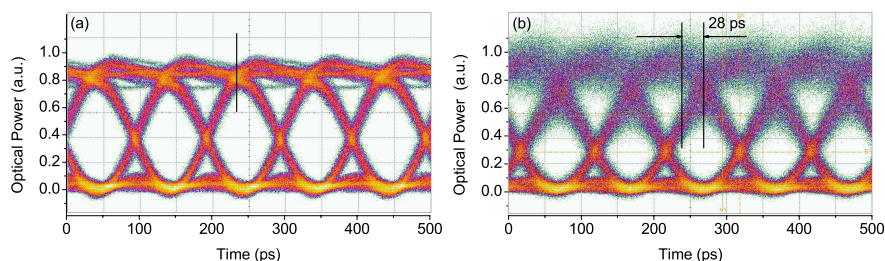


Fig. 6. Eye diagrams of pseudo-random bit sequence in the (a) absence and (b) presence of the pump laser with a power of 160 mW.

tion ($\text{BER} < 10^{-9}$). The MZM (EOspace, 12 Gb/s) is driven by a PRBS generated by a Pattern Generator (HP 70004A) to create the optical input sequence. An optical modulator driver (JDS, H301-1110) is used to increase the amplitude of the modulation. We use the 9.2-GHz gain profile shown in Fig. 5(a). The power reaching the photodetector (NewFocus, 1544B, 1 mW maximum input power) is kept constant in all the measurements using a variable attenuator placed before the receiver. An Error Performance Analyser (Agilent, 70843B, 0.1-12 Gb/s) is used to measure the BER. With this device, we were not able to directly measure the slow-light delay of the data stream. Therefore, we use a 8-GHz oscilloscope (Agilent, DSO80804B) to measure the delay. Although the limited bandwidth of the oscilloscope distorts the pseudo-random bit sequence, we find that the temporal position of the maximum eye opening, and thus the delay, can be determined accurately as verified by numerical simulations of our system.

BER performance is mainly degraded by the noise introduced by the Rayleigh backscattering and by the filtering effect of the limited gain bandwidth. We use an input signal power of up to 12 dBm to reduce the former cause of degradation while the flat top SBS gain profile reduces the latter while improving the delay, as discussed in Sec. 2. Figure 6 shows the eye diagram for the output and input sequences for an input pump power of 160 mW, which corresponds to a maximum *small-signal* SBS gain of 13 dB. The maximum delay under free-error operation is 28 ps which was achieved for this input pump power. This result is below the 35 ps delay time achieved with error-free operation by Yi *et al.* in [14].

In our experiment, we believe that the optical input sequence is already somewhat distorted (just below a BER of 10^{-12} , the limit of the BER analyzer. Thus, relatively low distortion by the slow-light channel raises the error above the error-free threshold. In addition, Rayleigh backscattering of the pump light may contribute to the noise seen in Fig. 6, which degrades the BER. This scattered light could be partially removed using a spectral filter before the photodetector. Besides that, other modulation formats, such as PSBT or DPSK, have shown to provide better performance due to higher dispersion tolerance and spectral efficiency [14, 25]. Finally, an optimized profile based on other distortion metrics such as eye-opening or power penalty could provide better results, as pointed out in [15].

5. Conclusions

We have obtained an optimized SBS gain profile to achieve large delay of 10 Gb/s signals while minimizing the pulse distortion. To obtain the profile, measurements of the instantaneous frequency evolution of the pump laser are performed. These measurements are used to design an optimal waveform to modulate the injection current of the pump laser to obtain a flat top gain

profile. Delay and distortion performance are measured showing delays up to 3 times the input pulse width while keeping the output-to-input pulse-width ratio below 1.8 when an optimum gain profile with a 7.2 GHz bandwidth is used. The fractional delay reaches a value of 2.1 with a corresponding output-to-input pulse-width ratio of 1.3 when the gain bandwidth is increased to 9.2 GHz. Bit-error-rate measurements of an amplitude-modulated NRZ signal show error-free operation up to a delay time of 28 ps.

Acknowledgments

E.C.-G. and D.J.G gratefully acknowledge the support of the DARPA DSO Slow Light program. E.C.-G. also acknowledges the support of Fundación Ramón Areces. O.G.C. and S.M. acknowledge the support of the projects FIS2007-65382 (MEC) and PR34/07-15847 (UCM/BSCH).